PERGAMON

Planetary and Space Science 49 (2001) 395–404

Planetary and Space Science

www.elsevier.nl/locate/planspasci

Enhanced phase space diffusion due to chaos in relativistic electron–whistler mode wave particle interactions with applications to Jupiter

W.J. Wykes *, S.C. Chapman, G. Rowlands

Space and Astrophysics Group, University of Warwick, Conventry CV4 7AL UK

Received 9 November 1999; received in revised form 29 May 2000; accepted 19 June 2000

Abstract

Using numerical solutions of single-particle dynamics, we consider a chaotic electron–whistler interaction mechanism for enhanced diffusion in phase space. This process, when applied to parameters consistent with the Jovian magnetosphere, is a candidate mechanism for pitch angle scattering in the Io torus, thus providing a source of auroral precipitating electrons. We initially consider the interaction between two oppositely directed monochromatic whistler mode waves. We generalize previous work to include relativistic effects. The full relativistic Lorentz equations are solved numerically to permit application to a more extensive parameter space. We use this simplified case to study the underlying behaviour of the system. For large-amplitude monochromatic waves the system is stochastic, with strong diffusion in phase space. We extend this treatment to consider two oppositely directed, broad band whistler wave packets. Using Voyager 1 data to give an estimate of the whistler wave amplitude at the Io torus at Jupiter, we calculate the degree of pitch angle scattering as a function of electron energy and initial pitch angle. We show that for relatively wide wave packets, significant pitch angle diffusion occurs (up to $\pm 25^{\circ}$), on millisecond timescales, for electrons with energies from a few keV up to a few hundred keV.

Keywords: Relativistic; Chaos; Whistler; Pitch angle diffusion; Substorms

1. Introduction

The electron–whistler interaction has been considered as a potential mechanism for pitch angle scattering in planetary magnetospheres. Whistler waves are able to resonate with electrons over a broad energy range, from less than 100 keV to several MeV (Horne and Thorne, 1998). In particular, the Hamiltonian has been obtained for relativistic electrons interacting with a whistler mode wave of single $\hat{\mathbf{k}}$, revealing underlying behaviour that is dynamically simple (Laird, 1972).

Gyroresonance processes with near parallel propagating whistler waves have been considered as a pitch angle scattering mechanism (e.g. Kennel and Petschek, 1966; Lyon and Williams, 1984). These processes consider electrons at resonance with many whistler waves of different frequencies to produce pitch angle diffusion (Gendrin, 1981). Instead we consider a process that is enhanced over (and in addition to) 'diffusion' associated with particle dynamics strictly at resonance. We consider a stochastic interaction mechanism, for which particles, that are not at resonance with the waves, effectively diffuse faster than the particles that are in resonance. For clarity, we will refer to this as 'off-resonance' diffusion.

Stochasticity has been introduced by coupling the bounce motion of the trapped electrons with a single whistler (Faith et al., 1997), while the presence of a second, oppositely directed whistler wave was shown from the non-relativistic equations of motion to introduce stochasticity into the system, demonstrated numerically for a wave frequency of half the electron gyrofrequency by Matsoukis et al. (1998). This mechanism has been shown to exist in self-consistent simulations (Devine and Chapman, 1996). Diffusion processes are also effected by inhomogeneities in the medium (see, for example, Helliwell and Katsufrakis, 1974) though in the case considered here variations in the background field over the short-distances travelled by the electrons during the rapid

* Corresponding author. Tel.: +44-24-76522831; fax: +44 (0)24 76692016.

E-mail address: wykes@astro.warwick.ac.uk (W.J. Wykes).

0032-0633/01/$ - see front matter
PII: S0032-0633(00)00160-4

interaction are small and the background magnetic field can be assumed to be uniform.

Wave propagation calculations by Wang et al. (1995) have shown that lightning induced whistlers are guided into the Io torus by the strong local peaks in density. The waves tend to oscillate around the field line corresponding to the peak in torus density ($L = 5.7$, Wang et al., 1995), in a similar way to ducted whistlers with low normal angles ($\leqslant 10^\circ$) at the equator. We consider the interaction of two oppositely directed whistlers with the same frequency, propagating parallel to the background field, since small differences in the wave frequencies and slightly oblique waves (wave normal $\leqslant 10^\circ$) result in small perturbations to the dynamics of the system.

In this paper we generalize the work of Matsoukis et al. (1998) to consider a range of wave frequencies below the gyrofrequency and include relativistic effects. We consider the efficiency of the mechanism in scattering electrons in 'pancake distributions', i.e. distributions with a large peak in the distribution function at 90° pitch angles (sometimes represented as $T_\perp \gg T_{||}$). Since we are considering single-particles dynamic over a range of phase space, and not the evolution of the distribution function, per se, we study pancake distributions by considering electrons with high initial pitch angles, i.e. $v_\perp > v_{||}$. These then evolve to explore phase space. Recent plasma density models have shown that anisotropic distributions are required to fit the observed whistler dispersions in the Jovian magnetosphere (Crary et al., 1996). We investigate the dependence of the degree of stochasticity of the system (using Lyapunov exponents) on the wave amplitude, wave frequency and perpendicular velocity.

We simplify the equations of motion in the limit of low wave amplitudes and extend the process to study two oppositely directed, broad band whistler wave packets. We obtain an estimate for the whistler wave amplitude using the analysis of Voyager 1 data (see Scarf et al., 1979; Kurth et al., 1985; Hobara et al., 1997) and estimate the degree of pitch angle scattering for different electron energies resulting from the interaction with wave packets of different bandwidths.

2. Equations of motion

We consider a total magnetic field of the form

$$\mathbf{B} = \mathbf{B}_0 + \mathbf{B}_\omega^+ + \mathbf{B}_\omega^-,$$

where $\mathbf{B}_0 = B_0\hat{\mathbf{x}}$ is the background magnetic field and $\mathbf{B}_\omega^+$ and $\mathbf{B}_\omega^-$ are the whistler waves propagating parallel and anti-parallel to the background field, respectively (for coordinate system see Fig. 1). We assume that the background field lines are uniform, since, as we will see, the interaction is sufficiently fast so that changes in the background field experienced by the electrons are small, e.g., for electrons close to Jupiter's magnetic equator at $6R_J$, the field changes

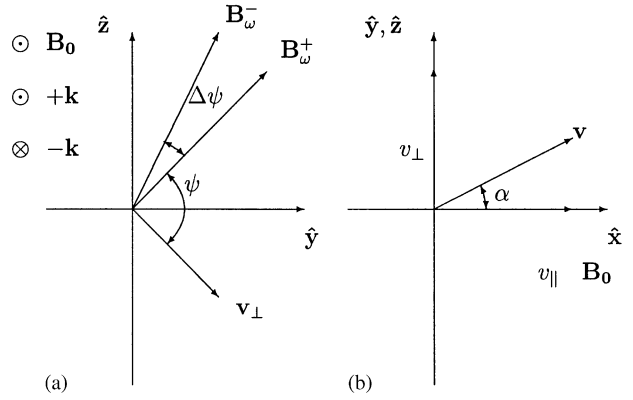

Fig. 1. Illustration of the coordinate system used in the model. In (a) the magnetic wavefields $\mathbf{B}_\omega^+$ and $\mathbf{B}_\omega^-$ lie in the $\hat{\mathbf{y}}, \hat{\mathbf{z}}$ plane, perpendicular to the background field, $\mathbf{B}_0 = B_0\hat{\mathbf{x}}$. The phase angle ψ is defined as the angle between $\mathbf{B}_\omega^+$ and the electron perpendicular velocity, $\mathbf{v}_\perp$ and $\Delta\psi$ is the angle between $\mathbf{B}_\omega^+$ and $\mathbf{B}_\omega^-$. In (b) the electron pitch angle α is defined as the angle between the velocity vector $\mathbf{v}$ and the background field $\mathbf{B}_0$.

by less than 1% for an MeV electron travelling at $0.9c$ and interacting with the field for 1000 electron gyroperiods (0.1 s).

The wavefields $\mathbf{B}_\omega^+$ and $\mathbf{B}_\omega^-$ are given by

$$\mathbf{B}_\omega^+ = B_\omega[\cos(kx - \omega t)\hat{\mathbf{y}} - \sin(kx - \omega t)\hat{\mathbf{z}}],$$

$$\mathbf{B}_\omega^- = B_\omega[\cos(-kx - \omega t + \theta_0)\hat{\mathbf{y}} - \sin(-kx - \omega t + \theta_0)\hat{\mathbf{z}}]$$

with $\hat{\mathbf{x}}$ parallel to the background field and $\hat{\mathbf{y}}$ and $\hat{\mathbf{z}}$ perpendicular. The wave amplitude is given by B_ω, while $\theta_0 = \pi$ is the initial phase difference of the waves. The wave frequency, ω, and wave number, k, are given by the electron whistler mode dispersion relation (neglecting ion effects):

$$\frac{k^2c^2}{\omega^2} = 1 - \frac{\omega_{pe}^2}{\omega(\omega - \Omega_e)}, \tag{1}$$

where ω_{pe} is the plasma oscillation frequency and Ω_e is the electron gyrofrequency. Electrons travelling at the correct parallel velocity will experience a constant field and will interact strongly with it. This resonance velocity, $\mathbf{v}_r = v_r\hat{\mathbf{x}}$ is given by the resonance condition:

$$\omega - \mathbf{k}\cdot\mathbf{v}_r = n\Omega_e/\gamma, \tag{2}$$

where n is an integer, and $\gamma = (1 - v^2/c^2)^{-1/2}$ is the relativistic factor. The corresponding electric field is obtained from Maxwell's relation for plane propagating waves, $k\mathbf{E}_\omega = \omega\hat{\mathbf{k}}\wedge\mathbf{B}_\omega$ and the dispersion relation (1).

We write $\mathbf{v} = v_{||}\hat{\mathbf{x}} + v_\perp\cos\phi\hat{\mathbf{y}} + v_\perp\sin\phi\hat{\mathbf{z}}$, where $\phi = \phi(t)$ is the phase of the perpendicular velocity, define the phase angle $\psi = kx - \omega t + \phi$ as the angle between the perpendicular velocity and $\mathbf{B}_\omega^+$ and define the phase difference $\Delta\psi = \theta_0 - 2kx$ as the angle between the two waves.

We substitute these into the Lorentz force law to give the full equations of motion:

$$\frac{\mathrm{d}v_{||}}{\mathrm{d}t} = \frac{bv_\perp}{\gamma}\left(1 - \frac{\omega v_{||}}{kc^2}\right)\sin\psi + \frac{bv_\perp}{\gamma}\left(1 + \frac{\omega v_{||}}{kc^2}\right)\sin(\psi + \Delta\psi), \tag{3}$$

$$\frac{\mathrm{d}v_\perp}{\mathrm{d}t} = -\frac{b}{\gamma}\left(v_{||} - \frac{\omega}{k}\left(1 + \frac{v_\perp^2}{c^2}\right)\right)\sin\psi - \frac{b}{\gamma}\left(v_{||} + \frac{\omega}{k}\left(1 + \frac{v_\perp^2}{c^2}\right)\right)\sin(\psi + \Delta\psi), \tag{4}$$

$$\frac{\mathrm{d}\psi}{\mathrm{d}t} = kv_{||} - \omega + \frac{1}{\gamma} - \frac{b}{\gamma v_\perp}\left(v_{||} - \frac{\omega}{k}\right)\cos\psi - \frac{b}{\gamma v_\perp}\left(v_{||} + \frac{\omega}{k}\right)\cos(\psi + \Delta\psi), \tag{5}$$

$$\frac{\mathrm{d}\gamma}{\mathrm{d}t} = \frac{b\omega v_\perp}{kc^2}\sin\psi - \frac{b\omega v_\perp}{kc^2}\sin(\psi + \Delta\psi), \tag{6}$$

where $b = B_\omega/B_0$ is wave amplitude scaled to the background field, and time and velocity have been rescaled with respect to the gyrofrequency, Ω_e, and the phase velocity, $v_\phi = w/k$, respectively. In the non-relativistic limit $\gamma \to 1$ these reduce to the non-relativistic equations of motion given in Matsoukis et al. (1998), (Eqs. (5)–(7)).

2.1. Reduced equations

We can reduce the full equations of motion (3)–(6) to demonstrate the underlying properties of the system for low wave amplitudes. The reduced equations also give qualitative information on how the system will be effected when different parameters are varied. To simplify the full equations of motion we rescale the velocities with respect to the normalized wave amplitude, b:

$$v_{||} = v_{||,0} + bv_{||,1}, \tag{7}$$

$$v_\perp = v_{\perp,0} + bv_{\perp,1}. \tag{8}$$

We substitute into Eqs. (3)–(6) and differentiate with respect to time. To first order in b, $v_{||,0}$ and $v_{\perp,0}$ are constant, $\gamma_0 = \sqrt{1 - v_{||,0}^2/c^2 - v_{\perp,0}^2/c^2}$ is a constant and we have $\psi = kx - (1/\gamma - \omega)t$, giving the following reduced equation:

$$\frac{\mathrm{d}^2x}{\mathrm{d}t^2} = \frac{2bv_{\perp,0}}{\gamma_0}\sin[(1/\gamma_0 - \omega)t]\cos[kx - \theta_0]. \tag{10}$$

Thus, we have the equation of a coupled pendulum with variables $v_{||} = \dot{x}$ and x. Perturbations in $v_{||}$ and x are proportional to the wave amplitude, b, to $1/\gamma_0$ and to $v_{\perp,0}$.

3. Wave packet approximation

The analysis of Voyager 1 data in Scarf et al. (1979) and Kurth et al. (1985) shows that whistler mode waves at the Io torus are broad band waves. Instead of a single pair of oppositely directed monochromatic whistler waves, we consider a sum of N such pairs, with each pair having a different frequency and (opposite) wave number. For N pairs of waves, the reduced equation (10) becomes

$$\frac{\mathrm{d}^2x}{\mathrm{d}t^2} = \sum_{i=1}^{N}\frac{2v_{\perp,0}}{\gamma_0}b_i\sin[(1/\gamma_0 - \omega_i)t]\cos[k_ix - \theta_0, i]. \tag{11}$$

As $N \to \infty$ we can replace the sum by an integral over ω:

$$\frac{\mathrm{d}^2x}{\mathrm{d}t^2} = \int_{-\infty}^{\infty}\frac{2v_{\perp,0}}{\gamma_0}A(\omega)\sin[(1/\gamma_0 - \omega)t] \times\cos[k(\omega)x - \theta_0(\omega)]\,\mathrm{d}\omega. \tag{12}$$

Where the wave amplitude function $A(\omega)$ is the wave amplitude per unit frequency bandwidth. We approximate the wave amplitude function using a 'top hat' distribution, i.e. we have a wave packet with central frequency, ω_0, and constant wave amplitude across a narrow range of wave frequencies, $\Delta\omega$:

$$A(\omega) = \begin{cases} 0, & \omega < \omega_0 - \dfrac{\Delta\omega}{2}, \\ A_0, & \omega_0 - \dfrac{\Delta\omega}{2} < \omega < \omega_0 + \dfrac{\Delta\omega}{2}, \\ 0, & \omega > \omega_0 + \dfrac{\Delta\omega}{2}. \end{cases} \tag{13}$$

We approximate the dispersion relation as $k(\omega) = k_0 + \beta(\omega - \omega_0)$, close to the central wave frequency, ω_0 and wave number, k_0, where $\beta = (3\omega_0^2 - 2\omega_0 - (\omega_{\mathrm{pe}}^2 + k_0^2c^2))/2k_0c^2(\omega_0 - 1)$, and $1/\beta$ is the group velocity of the wave packet. Substituting in and integrating with respect to the wave frequency, ω, gives the equation of motion for an electron interacting with two oppositely directed wave packets:

$$\frac{\mathrm{d}^2x}{\mathrm{d}t^2} = +\frac{2A_0v_{\perp,0}}{\gamma_0}\sin\left[\left(\frac{1}{\gamma_0} - \omega\right)t + k_0x\right] \times\frac{\sin[(t - \beta x)\Delta\omega/2]}{(t - \beta x)} + \frac{2A_0v_{\perp,0}}{\gamma_0}\sin\left[\left(\frac{1}{\gamma_0} - \omega\right)t - k_0x\right] \times\frac{\sin[(t + \beta x)\Delta\omega/2]}{(t + \beta x)}. \tag{14}$$

In the limit of narrow bandwidths, $\Delta\omega \to 0$, the wave packet equation (14) yields the reduced equation (10) with wave amplitude b_0. A more detailed derivation of the reduced equation (10), and the wave packet equation (14), can be found in Wykes et al. (2000).

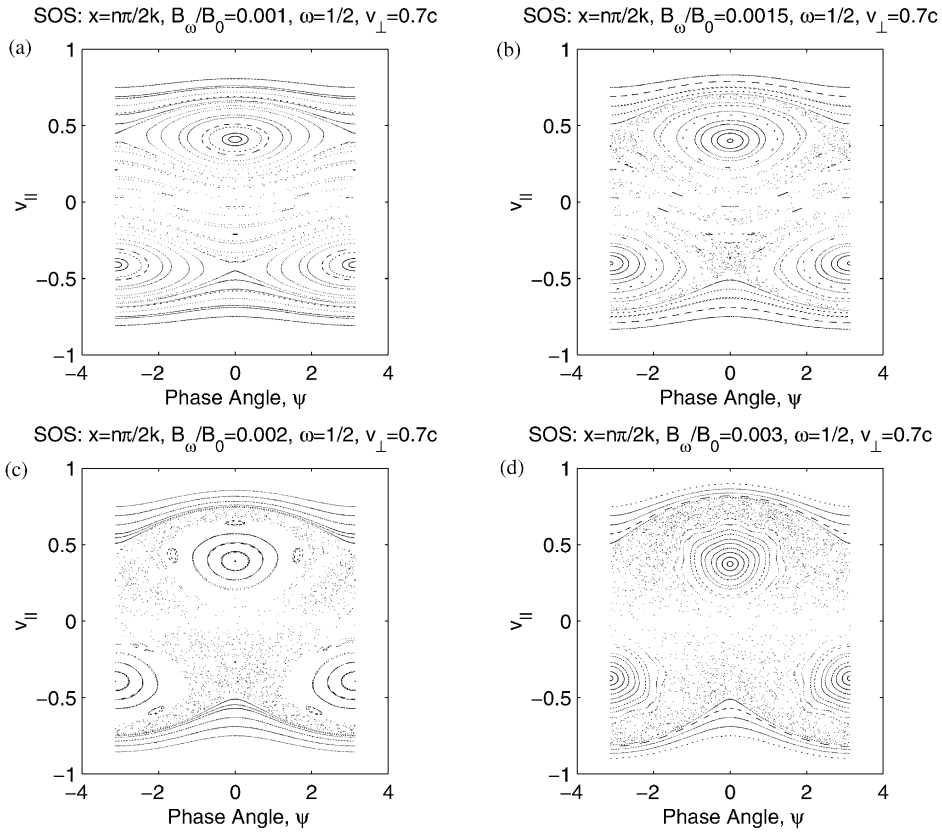

Fig. 2. Stroboscopic surface of section plots for $\omega/\Omega_e = 1/2$, initial $v_\perp = 0.7c$. The parallel velocity, $v_{||}$, has been scaled to the phase velocity, v_ϕ. For this wave frequency, the dispersion relation (1), gives $v_\phi = 0.07c$. The phase angle ψ is defined as the angle between the perpendicular velocity and the whistler wave propagating in the positive $\hat{\mathbf{x}}$ direction. For low wave amplitudes, panel (a), all trajectories are regular and the equations of motion reduce to a pendulum equation, with resonances given by the resonance condition (2). For slightly higher wave amplitudes, panels (b) and (c), stochastic effects appear as regular trajectories are broken down. For high wave amplitudes, panel (d), phase space is dominated by stochastic trajectories with regular trajectories confined to KAM surfaces close to the resonances. The stochastic region is bounded above and below by the first regular, untrapped, trajectories away from resonance, therefore there is a limit on the diffusion of electrons in phase space.

4. Numerical results

Fig. 2 shows numerical solutions of the full equations of motion. The phase diagrams are stroboscopic surfaces of section Tabor (1989) constructed from cut-planes where $x = (n+1/2)\pi/k$, to sample the full electron phase space. The initial parallel velocity, $v_{||}$, was varied over the range $[-v_r, v_r]$, where v_r is the resonance velocity, given by the resonance condition (2), to give a good coverage of phase space.

All electrons were given the same initial perpendicular velocity, $v_\perp = 0.7c$ ($v_\perp/v_r \approx 20$, to give high initial pitch angles in order to study a pancake distribution), and the phase angle, ψ (defined as the angle between the perpendicular velocity and the first whistler wave $\mathbf{B}^+_\omega$, see Fig. 1) was initially set to 0 or π.

For low wave amplitudes, Fig. 2(a), the trajectories are essentially regular and characterized by two sets of resonances. Regular trajectories are described by KAM surfaces (Tabor, 1989), i.e. the trajectories are near-integrable and there is an approximate constant of the motion associated with each orbit. The regular trajectories are represented in the phase diagrams as smooth lines.

As the wave amplitude is increased in Figs. 2(b) and (c), stochastic effects are introduced into the region between the two resonances (stochastic trajectories appear as a spread of dots). For higher wave amplitudes, Fig. 2(d), the system becomes increasingly stochastic with regular trajectories confined to KAM surfaces close to the resonances. The dependence of the degree of stochasticity on the wave amplitude is supported by the form of the reduced equation (10), where the perturbations in parallel velocity scale with the wave amplitude.

In Figs. 2(b)–(d), the stochastic regions are bounded by the first regular, untrapped, trajectories away from resonance. In Figs. 2(c) and (d), there are no regular trajectories separating the resonances and stochastic electrons can diffuse throughout the stochastic region, resulting in large changes in pitch angle. It can be seen that the stochastic electrons are able to diffuse to a greater extent in phase space than the electrons on regular trajectories.

In Fig. 3 we show a sequence of phase diagrams for increasing perpendicular velocity, with constant wave amplitude, $b = 0.003$, and wave frequency, $\omega = 1/2$. The reduced equation (10) describes pendulum like behaviour with

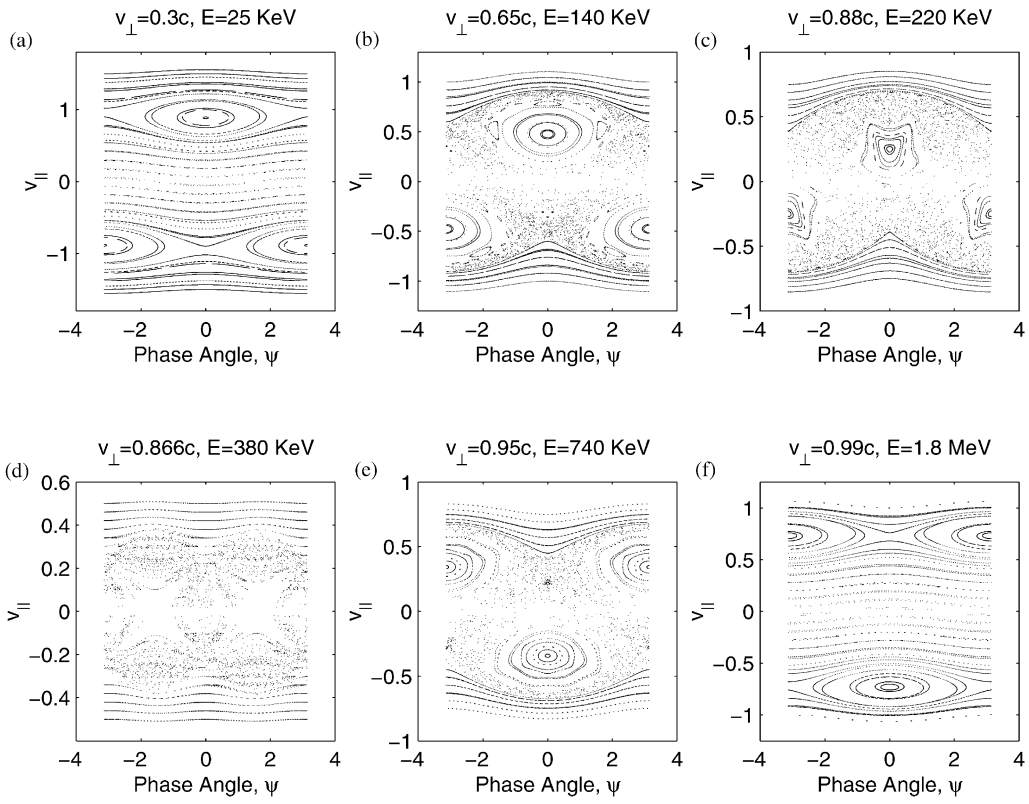

Fig. 3. Stroboscopic surface of section plots for $\omega/\Omega_e = 1/2$ and $b = B_\omega/B_0 = 0.003$. Electron energy increases as a function $v_\perp$. In panels (a)–(c) the degree of stochasticity increases with increasing perpendicular velocity (and electron energy, E) with constant ω, Ω_e, and k. As $v_\perp$ and γ increases the resonance velocity, v_r, decreases (see the resonance condition (2)). In panel (d) the resonance velocity is zero. Here $v_\perp = 0.86c$ and $E = 300$ keV. Increasing $v_\perp$ (and E) further in panel (e) causes the resonance velocities to cross the $v_{||} = 0$ line and the degree of stochasticity now decreases, until in panel (f) with $v_\perp = 0.99c$ ($E = 1.8$ MeV) the trajectories become regular once more.

oscillations in $v_{||}$ proportional to both the wave amplitude and the perpendicular velocity, $v_\perp$. The resonance condition (2) shows that $v_r = v_r(\gamma(v_\perp, v_{||}), k, \omega)$, therefore (for $v_{||} \ll v_\perp$) v_r, in addition to the total electron energy, E, can be described as a function of the perpendicular velocity when ω and k are constant. By varying $v_\perp$ only, we can consider the dependence of the degree of stochasticity on $v_\perp$ and hence E.

In Figs. 3(a) and (c), the perpendicular velocity increases to relativistic velocities, $v_\perp = 0.3$–$0.75c$ (energy 25–220 keV). The degree of stochasticity increases with $v_\perp$. From the resonance condition (2) we see that increasing $v_\perp$ increases γ and hence reduces v_r and the separation between the two resonances.

In Fig. 3(d) where $v_\perp = \sqrt{1-\omega^2} = 0.86c$ ($E = 380$ keV) the resonance condition (2) is satisfied for $v_r = 0$. Increasing $v_\perp$ further causes the resonances to pass through the $v_{||} = 0$ line and change sign. In Fig. 3(e) we have $v_\perp = 0.95c$ ($E = 740$ keV). The resonance velocity now increases with $v_\perp$ and the degree of stochasticity decreases, until the system is no longer dominated by stochastic trajectories (Fig. 3(f)) with $v_\perp = 0.99c$, $E = 1.8$ MeV).

The presence of a peak in the degree of stochasticity and its dependence on $v_\perp$ is a relativistic effect. For non-relativistic velocities, γ, and hence the resonance velocity, is constant and the degree of stochasticity continually increases with $v_\perp$ (Matsoukis et al., 1998).

In Figs. 4 and 5 we show phase diagrams similar to Fig. 2 except that we now plot pitch angle against phase angle. The initial conditions are; $b = 0.003$, $\omega = 1/2$, $v_\perp = 0.7c$ and $E = 175$ keV. The phase diagrams are qualitatively similar to Fig. 2 and share many of the same features. Regular trajectories are confined to close to the resonance pitch angle, $\alpha_r = \arctan(v_{\perp,0}/v_r)$, where $v_{\perp,0}$ is the initial perpendicular velocity ($0.7c$) and v_r is the resonance velocity. The stochastic region is bounded by the first regular, untrapped, trajectories away from resonance. Again, we see that stochastic electrons are able to diffuse in pitch angle to a greater extent than resonant electrons. Later, we shall investigate the change in pitch angle for wave amplitudes obtained for the Jovian magnetosphere, as a function of electron energy, initial pitch angle and wave frequency.

In Fig. 5 diffusion in pitch angle is very fast. Significant pitch angle diffusion occurs on timescales of the order of tens of electron gyroperiods. On these timescales, electrons at Jupiter's magnetic equator ($L = 6$), travelling parallel to the background magnetic field at high relativistic velocities ($v \approx c$), experience changes in the background magnetic

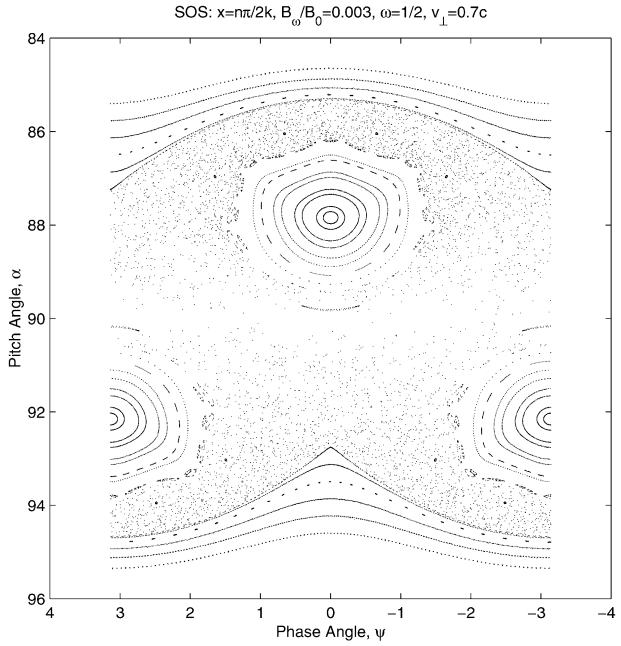

Fig. 4. Pitch angle plotted against phase angle for $b = 0.003$, $\omega/\Omega_e = 1/2$, $v_\perp = 0.7c$ and $E = 175$ keV. Phase space is divided into stochastic and regular regions in a similar way to Fig. 2. Electrons with regular trajectories close to the velocity resonances in Fig. 2 are confined to close to the resonance pitch angle $\alpha_r = \arctan(v_{\perp 0}/v_r)$. Pitch angle diffusion is limited by the extent of the stochastic region, which is bounded by the first untrapped orbit away from the resonances. The electrons that diffuse to the highest $v_{||}$ in Fig. 2 have the greatest change in pitch angle.

field of less then 1%, therefore the approximation that the background magnetic field is uniform is valid.

In Figs. 6(a) and (b) we show sample numerical solutions of the wave packet equation (14) for narrow wave packets ($\Delta\omega = \Omega_e/500$). In panel (a) there is little change in pitch angle with time and in panel (b) the trajectory is qualitatively similar to regular trajectories in Fig. 4. In Fig. 6(c), for wider wave packets, ($\Delta\omega = \Omega_e/50$), the change in pitch angle is greater ($\Delta\alpha \approx 15^\circ$, $\alpha_0 = 90^\circ$), with perturbations in pitch angle decreasing with time. The trajectory in panel (d) is similar to stochastic trajectories in Fig. 4.

We have investigated solutions of the full equations of motion in order to understand the underlying behaviour of the system. We now consider numerical solutions of the more realistic wave packet equation for applications to the Jovian magnetosphere.

5. Estimation of whistler wave amplitudes

We use the analysis of Voyager 1 data in Scarf et al. (1979); Kurth et al. (1985) and Hobara et al. (1997) to estimate the whistler wave amplitude. For the Io torus at Jupiter the electron gyrofrequency, $\Omega_e = 334$ kHz, corresponding to a background field, $B_0 = 1900$ nT. At $L = 6$ the plasma frequency, $\omega_{pe} = 2230$ kHz (see Scarf et al., 1979; Kurth et al., 1985). We consider broad band whistlers with frequencies up to the electron gyrofrequency and bandwidths of the order of a few kHz ($\Delta\omega = \Omega_e/50$, see Hobara et al., 1997).

The plasma wave instrument on Voyager 1 measures the electric field spectral density ($E^2_\omega/\Delta\omega$) of the whistler waves over a set of frequency channels of finite width $\Delta\omega$. We estimate the corresponding magnetic field strength using:

$$B_\omega = \frac{E_\omega}{v_\phi},$$

where $v_\phi = \omega/k$ is the phase velocity given by the dispersion relation (1). Using a spectral density of 10^{-11} V^2 m^{-2}/Hz obtained by Hobara et al. (1997) we obtain a wave amplitude, $b = B_\omega/B_0 = 10^{-5}$ and a wave amplitude function $A_0 = B_\omega/\Delta\omega = 10^{-3}$ for a wave frequency, $\omega = \Omega_e/2$. While this is insufficient for stochasticity for a single pair of monochromatic whistlers, for broad band whistler wave packets, significant diffusion does occur.

We obtain a similar estimate using Ulysses data for the Jovian magnetopause (Spectral density $= 10^{-12.8}$ V^2 m^{-2}/Hz for $\omega = \Omega_e/2$, see Tsurutani et al. (1997)). To determine uniquely whether or not this process is significant, for a given bandwidth, wave amplitude rather than spectral density measurements are needed.

In this context it interesting to note that for the Earth, direct amplitude measurements ($b = 5 \times 10^{-4}$, see Nagano et al., 1996) and the extrema of spectral density measurements ($b = 5 \times 10^{-3}$, see Parrot and Gaye, 1994) yield whistler amplitudes sufficient for stochasticity with a pair of monochromatic whistlers, whereas average spectral density measurements do not (Tsurutani et al., 1989).

5.1. Pitch angle diffusion in the Io torus at Jupiter

In Fig. 7 we plot the change in pitch angle for electrons during an interaction with two oppositely directed whistler wave packets with relatively wide bandwidths ($\Delta\omega = 10$ kHz, see Hobara et al., 1997), central wave frequency, $\omega_0 = \Omega_e/2$, and wave amplitudes consistent with the Jovian magnetosphere ($A_0 = 10^{-3}$). We estimate the change in pitch angle for electron trajectories with initial pitch angles in the range $\alpha_0 = [0^\circ, 180^\circ]$ and electron energies from 0 to 400 keV. Significant pitch angle diffusion occurs, from a few degrees for low initial pitch angles, up to 25° for higher initial pitch angles, for a range of electron energies.

Increasing the central wave frequency has the effect of shifting the entire structure shown in Fig. 7 down in energy. Lower wave frequencies are required to efficiently scatter high-energy electrons ($E > 1$ MeV). Given an even distribution of waves with frequencies up to the electron gyrofrequency, electrons with energies from a few keV up to a few hundreds of keV are most readily scattered. The pitch angle diffusion mechanism described above is consistent with the

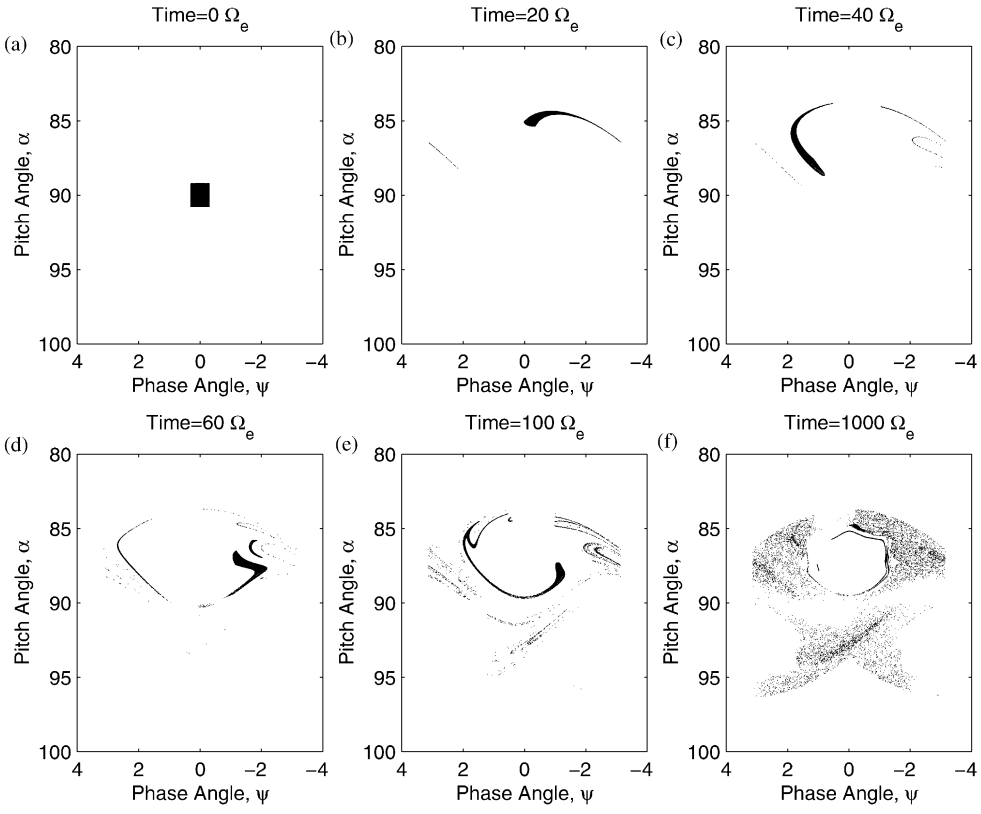

Fig. 5. Series of phase plots showing diffusion in pitch and phase angle for a small set of initial conditions. Diffusion is rapid with electrons reaching the minimum pitch angle in tens of electron gyroperiods. After 100 electron gyroperiods, electrons have diffused throughout the stochastic region. Parameters are as in Fig. 4.

framework described by Kennel and Petschek (1966). However, in their derivation of the diffusion coefficient (see their Eqs. (3.6)–(3.10)) they make an estimate of the timescale for diffusion based on the dynamics of particles near resonance. Here, we examine the detailed dynamics in phase space and find that particles off resonance are chaotic and as a consequence diffuse much faster than estimated by Kennel and Petschek (1966). Hence we have termed this process 'off-resonance' diffusion.

5.2. Lyapunov exponents

Lyapunov exponents are used to quantify the degree of stochasticity in the system. The Lyapunov exponents are calculated using the method described by Benettin et al. (1976) and Parker and Chua (1989). All six Lyapunov exponents were calculated over phase space and evolved to their asymptotic limit. The only significant Lyapunov exponent corresponds to the coordinate directed along the background field.

For positive Lyapunov exponents, two trajectories that are initially close together in phase space will diverge exponentially in time. For negative or zero Lyapunov exponents, two trajectories that are initially close together in phase space will remain close together. Positive (negative) Lyapunov exponents correspond to stochastic (regular) trajectories in phase space. For a detailed description of the theory of Lyapunov exponents see Hilborn (1994).

In Fig. 8 we plot the Lyapunov exponent for 10 keV electrons, averaged over a series of trajectories with pitch angles in the range $[0^\circ, 180^\circ]$. We consider the interaction between electrons and two oppositely directed whistler wave packets with relatively wide bandwidths ($\Delta\omega = 10$ kHz, see Hobara et al. (1997)) and investigate the dependence of the Lyapunov exponent on the relativistically correct wave frequency, $\omega_\gamma = \gamma\omega$. The Lyapunov exponents are plotted as a function of $1/\omega_\gamma$. The Lyapunov exponent is enhanced when $\omega_\gamma = 1/n$, where n is an integer. It then follows that close to these frequencies the process will be the most efficient in pitch angle scattering. The structure in the dependence of the Lyapunov exponent on the relativistically correct wave frequency is subtle and arises from higher-order terms in the reduced equation (10).

The separation of two electrons, with Lyapunov exponent λ, in phase space, scales approximately as $\sim \exp \lambda t$, thus an order of magnitude estimate shows that changes in pitch angle scale approximately as $\sim \exp \lambda t$, giving a characteristic time constant, τ, for changes in pitch angle of by a factor of

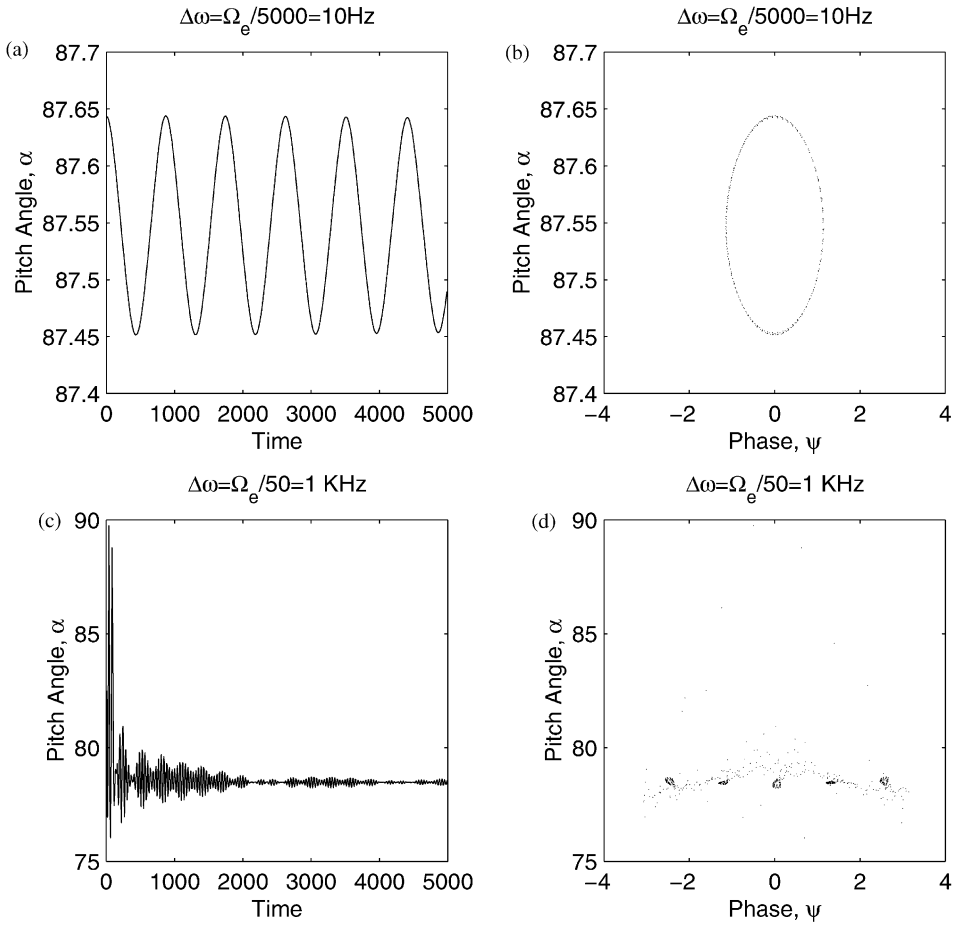

Fig. 6. Changes in pitch angle for sample solutions of the wave packet equation for two widths of wave packet. In panels (a) and (b) $\Delta\omega=\Omega_e/5000=100$ Hz resulting in very narrow wave packets. Trajectories are regular and resulting changes in pitch angle are low. In panels (c) and (d) $\Delta\omega=\Omega_e/50=10$ kHz, with initial pitch angle $\alpha(t=0)=90^\circ$. The trajectories are now stochastic, with greater change in pitch angle. In panel (c) it can be seen that perturbations in the parallel velocity decrease with time.

e^1, of approximately τ/λ gyroperiods. Thus the Lyapunov exponents in Fig. 8 indicate changes in pitch angle occurring in tens of electron gyroperiods.

6. Discussion

We have considered the interaction between two oppositely directed whistler waves and relativistic electrons. We initially considered monochromatic whistlers in order to understand the underlying behaviour of the system. For whistlers with wave amplitudes consistent with the Jovian magnetosphere the interaction with two oppositely directed monochromatic whistler waves results in weak diffusion in phase space. Stochastic effects can be introduced with high wave amplitudes: electrons not in resonance with either of the two whistlers can diffuse extensively in phase space. We refer to this process as 'off-resonance' diffusion as only the electrons not in resonance are scattered in this way. Resonance diffusion remains unchanged.

We have extended the treatment of monochromatic whistlers to consider two oppositely directed whistler wave packets. For relatively broad band waves with amplitudes consistent with quiet times in the Jovian magnetosphere, we have shown that the 'off-resonance' diffusion results in significant pitch angle diffusion (up to 25°) on timescales of the order of a few tens of electron gyroperiods (milliseconds). 'Off-resonance' diffusion is most effective in scattering electrons with energies from a few keV up to a few hundred keV (MeV electrons require extremely low wave frequencies for effective scattering).

We have shown that the Lyapunov exponent is enhanced when the relativistically correct wave frequency $\omega_\gamma = \gamma\omega = 1/n$ where $n = 1, 2, 3, \ldots$. This phenomenon arises purely from the interaction of the two whistler waves. We expect enhanced phase space diffusion close to these frequencies.

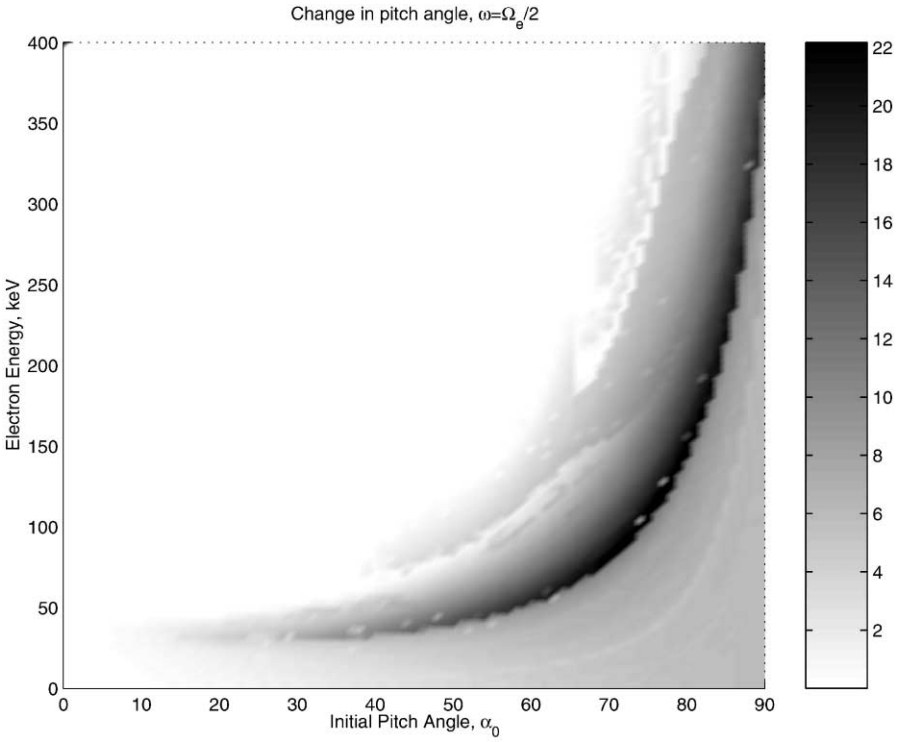

Fig. 7. Pitch angle diffusion for relatively wide, oppositely directed whistler wave packets ($\Delta\omega = \Omega_e/50$) with central frequency $\omega = \Omega_e/2$ and low wave amplitude ($A_0 = 10^{-3}$). We plot the change in pitch angle against initial pitch angle and electron energy. Significant pitch angle diffusion occurs (from a few degrees up to 25°) for a range of electron energies and initial pitch angles.

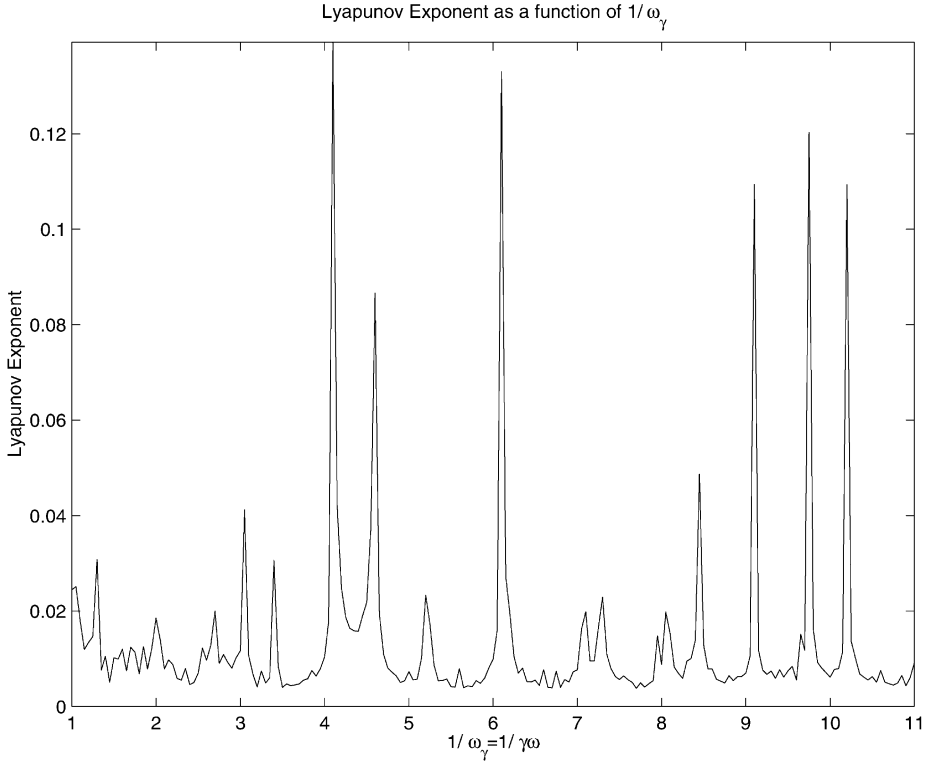

Fig. 8. We investigate the dependence of the Lyapunov exponent on the relativistically correct wave frequency $\omega_\gamma = \gamma\omega$, for relatively wide band whistler wave packets. We plot the Lyapunov exponent as a function of $1/\omega_\gamma$. The Lyapunov exponent is enhanced when $\omega_\gamma = 1/n$, where n is an integer.

Acknowledgements

W.J. Wykes and S.C. Chapman are funded by PPARC.

References

Benettin, G., Galgani, L., Strelcyn, J.M., 1976. Kolmogorov entropy and numerical experiments. Physica A 14, 2338.

Crary, F.J., Bagenal, F., Ansher, J.A., Gurnett, D.A., Kurth, W.S., 1996. Anisotropy and proton density in the Io plasma torus derived from whistler wave dispersions. J. Geophys. Res. 101, 2699.

Devine, P.E., Chapman, S.C., 1996. Self-consistent simulation studies of non-linear electron–whistler wave–particle interactions. Physica D 95, 35.

Faith, J., Kuo, S., Huang, J., 1997. Electron precipitation caused by chaotic motion in the magnetosphere due to large-amplitude whistler waves. J. Geophys. Res. 102, 2233.

Gendrin, R., 1981. General relations between wave amplification and particle diffusion in a magnetoplasma. Rev. Geophys. 19, 171.

Helliwell, R.A., Katsufrakis, J.P., 1974. VLF wave-injection experiments into the magnetosphere from Siple Station, Antarctica. J. Geophys. Res. 79, 2571.

Hilborn, R.C., 1994. Chaos and Nonlinear Dynamics. Oxford University Press, Oxford.

Hobara, Y., Kanemaru, S., Hayakawa, M., 1997. On estimating the amplitude of Jovian whistlers observed by Voyager 1 and implications concerning lightning. J. Geophys. Res. 102, 7115.

Horne, R.B., Thorne, R.M., 1998. Potential waves for relativistic electron scattering and stochastic acceleration during magnetic storms. Geophys. Res. Lett. 25, 3011.

Kennel, C.F., Petschek, H.E., 1966. Limit on stably trapped particle fluxes. J. Geophys. Res. 71, 1.

Kurth, W.S., Strayer, B.D., Gurnett, D.A., Scarf, F.L., 1985. A summary of whistlers observed by Voyager 1 at Jupiter. Icarus 61, 497.

Laird, M.J., 1972. Cyclotron resonance in an inhomogeneous plasma. J. Plasma Phys. 8, 255.

Lyon, L.R., Williams, D.J., 1984. Quantitative Aspects of Magnetospheric Physics. D. Reidel, Hingham, MA.

Matsoukis, K.S., Chapman, S.C., Rowlands, G., 1998. Whistler mode wave coupling effects in the near Earth magnetosphere. Geophys. Res. Lett. 25, 265.

Nagano, I., Yagitani, S., Kojima, H., Matsumoto, H., 1996. Analysis of wave normal and poynting vectors of the chorus emissions observed by GEOTAIL. J. Geomagn. Geoelectr. 48, 299.

Parrot, M., Gaye, C.A., 1994. A statistical survey of ELF waves in geostationary orbit. Geophys. Res. Lett. 23, 2463.

Parker, T.S., Chua, L.O., 1989. Practical Numerical Algorithms for Chaotic Systems. Springer, New York.

Scarf, F.L., Coroniti, F.V., Gurnett, D.A., Kurth, W.S., 1979. Pitch-angle diffusion by whistler mode waves near the Io plasma torus. J. Geophys. Res. 6, 653.

Tabor, M., 1989. Chaos and Integrability in Nonlinear Dynamics — an Introduction. Wiley, New York.

Tsurutani, B., et al., 1989. A statistical study of ELF-VLF plasma waves at the magnetopause. J. Geophys. Res. 94, 1270.

Tsurutani, B., et al., 1997. Plasma wave characteristics of the Jovian magnetopause boundary layer: relationship to the Jovian Aurora?. J. Geophys. Res. 102, 4751.

Wang, K., Thorne, R., Horne, R., 1995. The propagation characteristics and Landau damping of Jovian whistlers in the Io torus. J.Geophys. Res. 100, 21 709.

Wykes, W.J., Chapman, S.C., Rowlands, G., 2000. Enhanced pitch angle diffusion due to stochastic electron–whistler wave–particle interactions. Phys. Plasmas, submitted for publication.